Bull. Mater. Sci. (2022)45:137
https://doi.org/10.1007/s12034-022-02714-4

Tetraphenylethylene-based fluorescent conjugated microporous polymers for fluorescent sensing trinitrophenol

LLYING REN[1] and TONGMOU GENG[2,*]

[1]Department of Pharmacy, Anqing Medical College, Anqing 246052, China
[2]AnHui Province Key Laboratory of Optoelectronic and Magnetism Functional Materials, School of Chemistry and Chemical Engineering, Anqing Normal University, Anqing 246011, China
*Author for correspondence (gengtongmou@sina.com)

MS received 15 January 2022; accepted 21 March 2022

Abstract. Two tetraphenylethylene-based fluorescent conjugated microporous polymers (TTTPT and TTDAT) were obtained by the Friedel–Crafts polymerization reactions catalysed by CH_3SO_3H. In virtue of containing tetraphenylethylene, triphenylamine and s-triazine units in their porous skeletons, the resulting TTTPT and TTDAT show excellent fluorescence sensing performance for trinitrophenol (TNP) with high quenching coefficients of 1.66×10^4 and 1.31×10^5 l mol^{-1}, respectively. TTDAT can also sense to dinitrophenol (DNP) with the K_{sv} of 2.70×10^4 l mol^{-1}. The fluorescent quenching mechanisms of TTTPT and TTDAT for selective detecting TNP attribute to conventional photoinduced electron-transfer mechanism, absorption competition quenching mechanism and/or the resonant energy transfer mechanism.

Keywords. Conjugated microporous polymer; fluorescence sensor; trinitrophenol; tetraphenylethylene; dinitrophenol.

1. Introduction

As one of nitro-aromatic compounds (NACs), 2,4,6-trinitrophenol (TNP) is a significant threaten for human health and national homeland safety [1]. TNP is not only one of the most dangerous explosives, but also severe environmental pollutant, and its extensive applications can cause hurt to the human body [2]. TNP can cause intense skin and eye irritation, severe respiratory disorders, liver or kidney damages, dizziness, as well as mutagenic effects, which give rise to significant menaces to mankind health [2–5]. It is also the cause of sycosis, anaemia, gastritis, cancer, infertility and diarrhea [5]. Because of the frequent use of TNP in fireworks, dyes, leather and textile industries, a fungicide in agricultural, a powerful explosive in landmines and pharmaceutical industries, TNP unavoidably leads to its release to the environment in the process of production and utilization, and brings about increased pollution of farmlands and water bodies [3,4,6]. As it is characterized by high water-soluble, strong toxicity and low biodegradability, which can cause serious pollution to the supply of irrigation land and groundwater, and has a harmful impact on human health, TNP has already been placed at the forefront pollutants [4,6]. Moreover, TNP has been considered an extremely dangerous explosive compared with other NACs, because of its low safety factor and high explosive energy [3,5,6]. Hence, fast, sensitive and selective detection TNP is important [3–6].

Among the various TNP determination methods, for instance, gas chromatography, liquid chromatography, mass spectrometry, Raman spectroscopy, cyclic voltammetry, ion mobility spectroscopy, ion mobility spectrometry, field-effect transistor and fluorescence spectroscopy [1,5–8], fluorescence sensing technique provides intriguing merits, for example, simplicity, excellent sensitivity, rapid response time, inexpensiveness, and it can test whether in solution or in solid-phase [3,5–10].

Several electron-rich conjugated microporous polymers (CMPs) have been successfully prepared and reported as chemosensors. In particular, fluorescent CMPs have been widely used in the study of NACs detection [7,10]. The microporous environment of the framework enables rapid diffusion of analytes, thus decreasing response time. The effective host-object interactions are valid to improve sensitivity [11]. The extended π-conjugate in CMPs can amplify signal transduction, hence further improving the sensitivity, which is known as the 'molecular wire effect' created by Swager group [5,9]. Furthermore, commercial NACs, for instance, TNP or dinitrophenol (DNP), all have the electron-withdrawing nitryl (–NO_2) that can interact with electron-donating CMPs, leading to effective excitation migration within the CMPs' porous structures to

Published online: 20 July 2022

improve quenching sensitivity. Therefore, these conjugated and porous features of the organic frameworks make CMPs suitable for detecting the NACs [8,9,12].

Our group [13] have developed two CMPs with the units of 1,3,5-triazine, triphenylamine (TPA) and tetraphenylethylene (TPE) (TTTPT and TTDAT, scheme 1). TTTPT and TTDAT are insoluble bulk solids and have the excellent porosity (564.8 and 44.1 $m^2\ g^{-1}$), high thermal stability (575 and 487°C) and excellent performances for fluorescence sensing and adsorbing I_2. As a continuation of the work, we studied the fluorescence sensing properties of TTTPT and TTDAT for TNP and DNP in the contribution.

2. Results and discussion

2.1 *Optical property*

As shown in the solid-state adsorption spectrograms of the both CMPs and their corresponding structural blocks [13], the significant redshifts of the maximum absorption peaks of TTTAT and TTDAT suggests that the conjugated performances were extended after polymerization reactions. When TTTPT and TTDAT are dispersed in some ordinary solvents, they emit strong fluorescence. TTTPT dispersion in 1,4-dioxane (DOX) shows the most robust fluorescence under light excitation at 460 nm wavelength, while TTDAT dispersion in DMF emit the maximum fluorescence upon excitation at 350 nm [13]. When they are excited at 365 nm, TTTPT dispersion in DOX and TTDAT dispersion in DMF radiate severally yellow-green and cyan fluorescence. The CIE chromaticity diagrams are identical to the fluotescence photographs of TTTPT and TTDAT (figure 1a and b) [14].

2.2 *Response time*

We studied the relationships between fluorescence intensities of TTTPT dispersion in DOX and TTDAT dispersion in DMF (1.0 mg ml^{-1}) and the time after addition of TNP (5.0×10^{-4} and 2.5×10^{-5} mol l^{-1}; figure 2). The fluorescence of TTTPT and TTDAT decreases almost instantly,

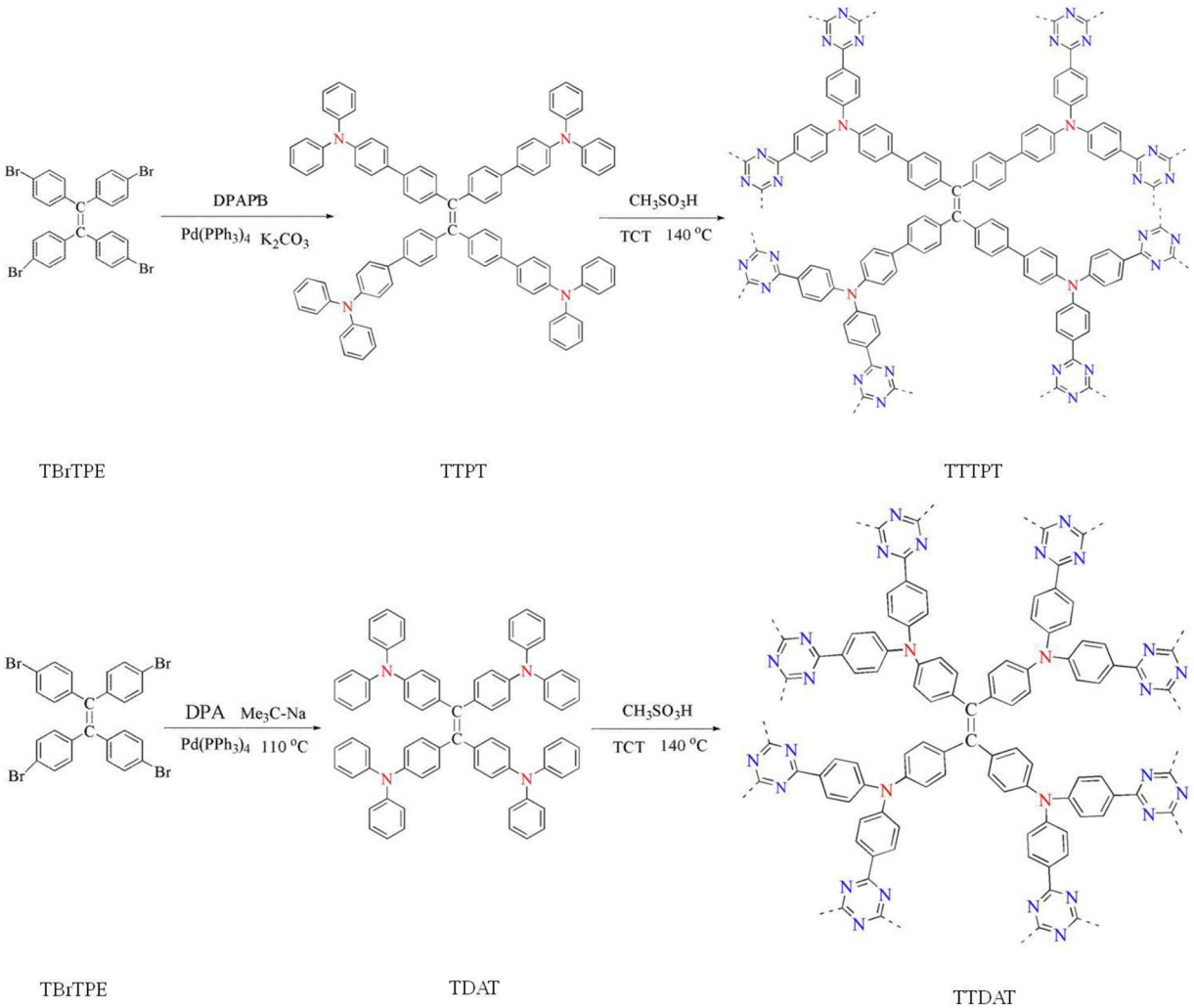

Scheme 1. Synthesis of TTTPT and TTDAT.

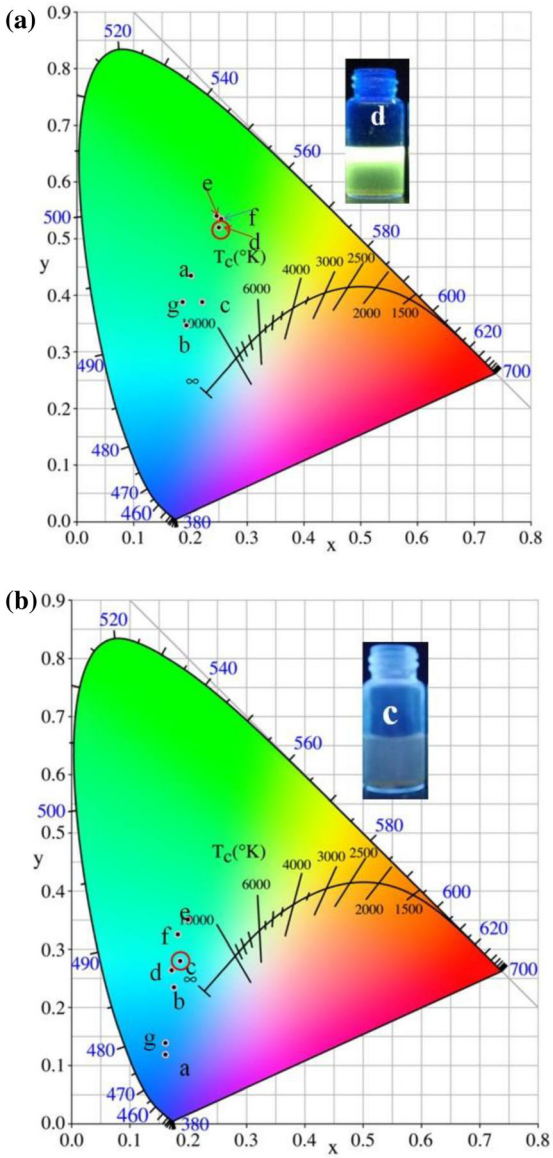

Figure 1. CIE chromaticity diagrams of (**a**) TTTPT and (**b**) TTDAT under ambient conditions, with excited wavelength 365 nm. Inserts: Photos of (**a**) TTTPT dispersed in DOX and (**b**) TTDAT dispersed in DMF under a UV lamp.

and reaches the quenching equilibrium in less than 20 s, which indicated that the porous networks and extended conjugate structure have fast responses to TNP [15,16]. The micropore structure can provide more sites of action for TNP and promote the rapid diffusion and proximity of TNP. Thus, the surface areas of CMPs improve the sensitivity in sensing to TNP and can shorten the response time [15–17].

2.3 *Sensitivity and selectivity*

Since TTTPT and TTDAT are porous and fluorescent, we then investigated their chemosensing behaviours by choosing the NACs, including TNP, p-nitrophenol (p-NP),

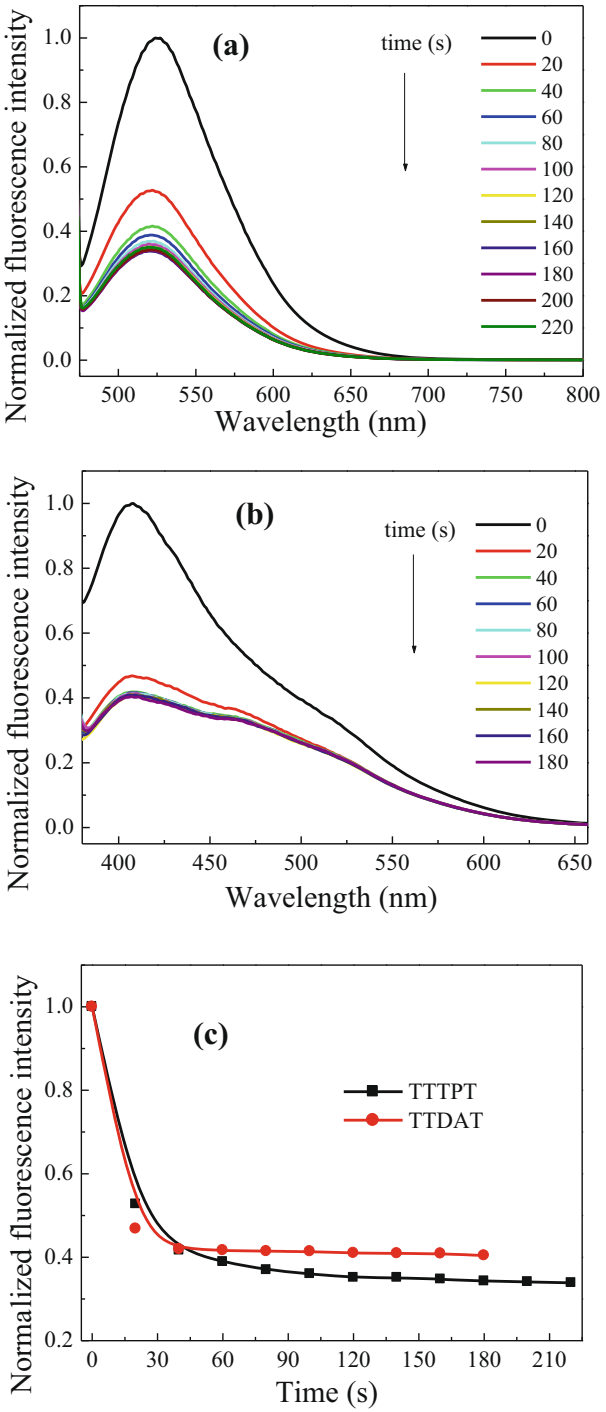

Figure 2. Normalized fluorescence intensities of the CMPs upon addition of TNP: (**a**) TTTPT, (**b**) TTDAT for different periods of time. (**c**) The plots of fluorescence maximum of TTTPT and TTDAT as the functions of time (1.0 mg ml^{-1}, TTTPT in DOX: excited at 460 nm; TTDAT in DMF: excited at 350 nm).

4-nitrotoluene (p-NT), nitrobenzene (NB), 2,4-dinitrotoluene (DNT), paradinitrobenzene (p-DNB), m-nitrobenzene (m-DNB), m-nitrophenol (m-NP), o-nitrophenol (o-NP), and DNP, as well as phenol (PhOH). Among them, the most toxic and damaging compounds, TNP and DNP,

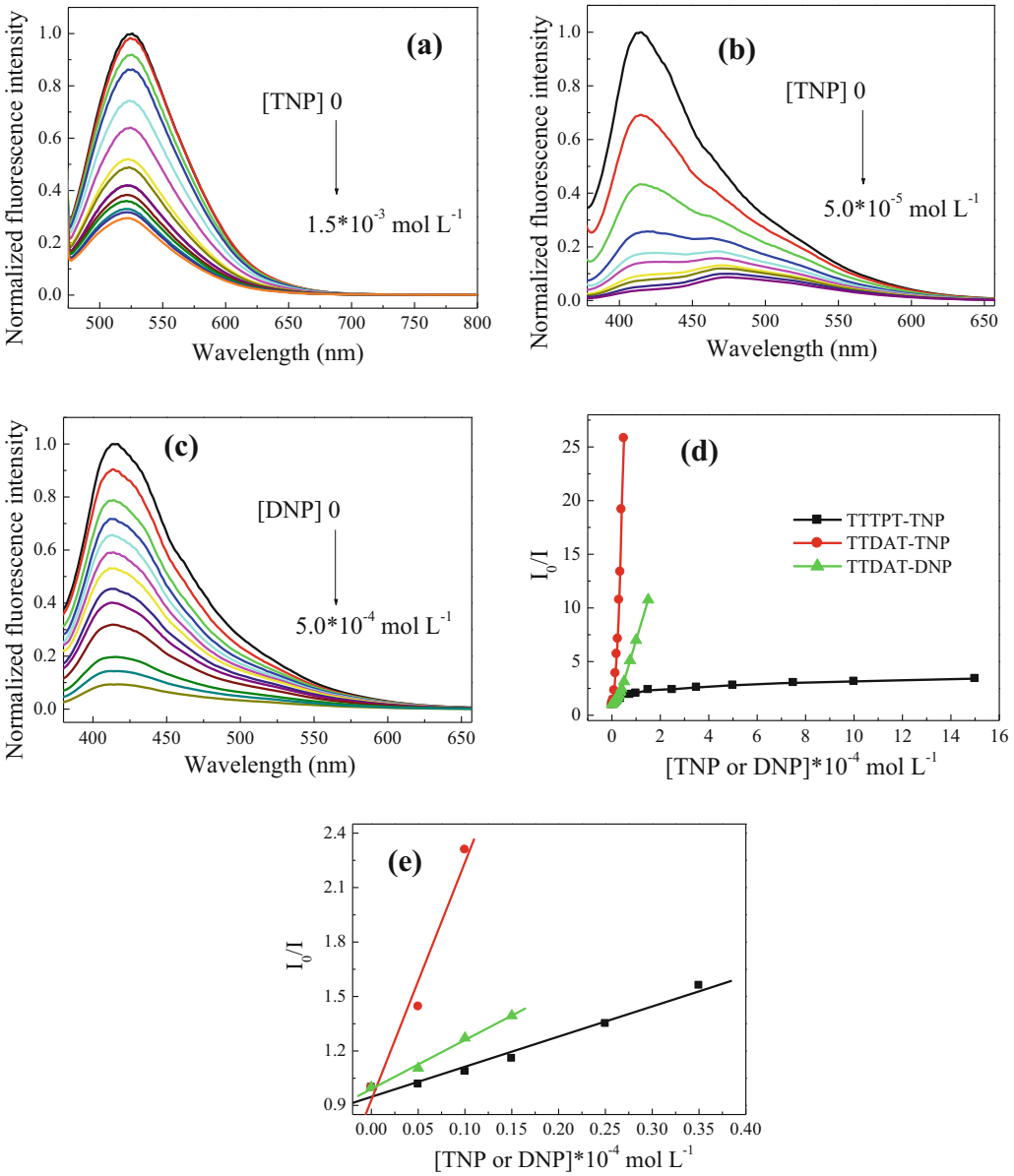

Figure 3. The changes of fluorescence spectra of the (**a**) TTTPT in dispersions of the DOX upon addition of TNP (1.0 mg ml^{-1}, excited at 460 nm); TTDAT in dispersions of the DMF upon addition of (**b**) TNP, (**c**) DNP (1.0 mg ml^{-1}, excited at 350 nm). Relative fluorescence intensity (I_0/I) of the (**d**) TTTPT and TTDAT in dispersions upon addition of various concentrations of TNP or DNP; (**e**) Stern–Volmer plots of TTTPT and TTDAT with various concentrations of TNP and DNP.

should deserve particular attention [18]. Figure 3a–c shows the fluorescence spectra of TTTPT and TTDAT with the incremental addition of different amounts of TNP and DNP into the dispersions of TTTPT in DOX and TTDAT in DMF. Apparently, the fluorescence of TTTPT and TTDAT was quenched when TNP was added gradually into the dispersions. When other NACs were added gradually into the dispersion, respectively, the quenching efficiencies were very low, indicating that TTTPT and TTDAT have good selectivity for TNP over other NACs [1,18,19]. We used the Stern–Volmer equation, $(I_0/I) = K_{SV}[A] + 1$, to calculate the quenching coefficients (or Stern–Volmer constants, K_{SV}) of TNP [18,20]. According to the Stern–Volmer curves, the K_{SV} values of TTTPT and TTDAT were estimated to be 1.66×10^4 and 1.31×10^5 l mol^{-1}, respectively (figure 3d and e, table 1), which are much bigger than those for other CMPs (table 2). Fluorescence spectrometric titration experiments proved that TTDAT can fluorescent sense DNP and has high sensitivity, and its K_{SV} reaches 2.70×10^4 l mol^{-1}. The limit of detections (LODs) of TNP in DOX for TTTPT and in DMF for TTDAT are severally 9.04×10^{-12} and 1.15×10^{-13} mol l^{-1} (table 1). The LOD

Table 1. Equation of I_0/I of TTTPT and TTDAT to the concentrations of TNP and DNP for suspension in DOX and DMF.

CMPs	Solvent	The equation	Regression coefficient (R)	The concentration range (mol l^{-1})	LODs (mol l^{-1})
TTTPT	DOX	$I_0/I = 0.9468 + 1.66 \times 10^4$ [TNP]	0.9870	0 to 3.5×10^{-5}	9.04×10^{-12}
TTDAT	DMF	$I_0/I = 0.9302 + 1.31 \times 10^5$ [TNP]	0.9834	0 to 1.0×10^{-5}	1.15×10^{-13}
TTDAT	DMF	$I_0/I = 0.9904 + 2.70 \times 10^4$ [DNP]	0.9966	0 to 1.5×10^{-5}	5.56×10^{-13}

Table 2. Summary of BET, K_{sv} and LODs of other CMPs for the determination of TNP.

Materials	BET ($m^2\ g^{-1}$)	K_{SV} (l mol^{-1})	LODs (mol l^{-1})	References
TDPDB	592.18	1.55×10^4	1.93×10^{-11}	[21]
CK-CMP	—	9.9×10^4	—	[12]
^{i}PrTAPB -Azo-COP	395	1.1×10^4	—	[5]
HPP-2	747	2.41×10^4	17.67 ppb	[7]
CMP-LS1	493	5.05×10^4	—	[10]
CMP-LS2	1576	3.70×10^4	—	
PNT-4	1311.54	6.22×10^5	2.36×10^{-9}	[2]
PNT-5	817.32	5.08×10^5	3.12×10^{-9}	
PNT-6	433.24	2.38×10^5	5.52×10^{-9}	
COP-612	48.80	2.51×10^5	—	[14]
DTF	705.27	2.08×10^3	7.22×10^{-7}	[22]
PTPATTh	594	5.00×10^3	3.01×10^{-9}	[15]
PTPATCz	894	4.28×10^3	7.01×10^{-9}	
TTPB	222.25	1.29×10^3	8.14×10^{-9}	[23]
DCZP	688	3.94×10^3	—	[24]
DCZN	97	6.63×10^3	—	
DBQP	355.76	9.02×10^4	3.33×10^{-13}	[25]
DBQN	25.48	1.79×10^4	2.48×10^{-13}	
COP-401	—	8.3×10^4	—	[26]
COP-301	—	2.6×10^5	—	
FL-SNWDPP-0.11	750	5.3×10^4	—	[18]
polyTPECz film	1020	6.4×10^4		[27]
COP-61	1302	2.40×10^5	1 ppm	[28]
COP-62	1208	1.82×10^5	1 ppm	
COP-63	931	8.04×10^4	1 ppm	
COP-64	716	9.79×10^4	1 ppm	
COP-65	869	6.80×10^4	1 ppm	
P2	39	2.1×10^3	—	[29]
P3	143	7.6×10^4	—	
COP-3	1869	1.45×10^4	—	[30]
COP-4	2015	3.93×10^3	—	
HHQ	24.16	2.30×10^5	1.30×10^{-11}	[31]
TTTPT	564.8	1.66×10^4	9.04×10^{-14}	This work
TTDAT	44.1	1.31×10^5	1.15×10^{-13}	

of DNP in DMF for TTDAT is determined to be 5.56×10^{-13} mol l^{-1}. These results showed that TTTPT and TTDAT in dispersions possess the high sensitivity for detecting TNP and DNP, and are comparable to other CMPs (table 2) [1,18,19,32]. The higher sensitivity of TTDAT to TNP than TTTPT to TNP is because the nitrogen content of TTDAT is higher than TTTPT, so that TTDAT has more sites of action with TNP than TTTPT. Thus, the sensitivities of CMPs to NACs fluorescence sensing depend their interactions with NACs rather than their specific surface areas.

The sensing selectivities of TTTPT and TTDAT systems to TNP were investigated (figure 4, red bar). 5.0×10^{-4} and 2.5×10^{-5} mol l^{-1} NACs (p-NP, TNP, NB, p-NT, o-NP,

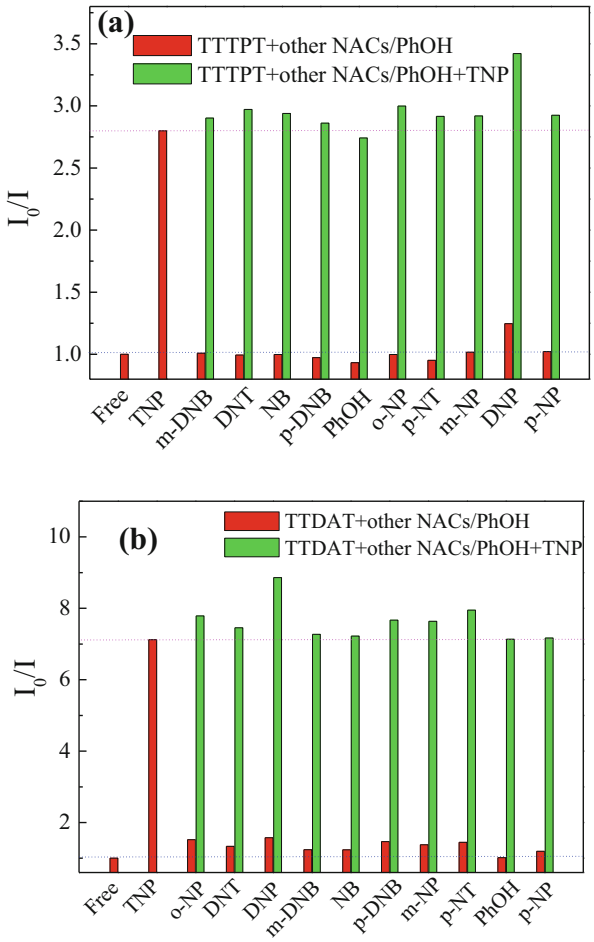

Figure 4. Selectivity and competitiveness of (**a**) TTTPT in DOX (the concentration of NACs and PhOH: 5.0×10^{-4} mol l^{-1}, λ_{ex} = 460 nm) towards TNP and (**b**) of TTDAT in DMF towards TNP (the concentration of NACs and PhOH: 2.5×10^{-5} mol l^{-1}, λ_{ex} = 350 nm). The red bars represent the relative fluorescent intensities of TTTPT and TTDAT in the presence of the competition NACs and PhOH, and the green bars represent the relative fluorescent intensity upon the addition of TNP to the above solutions.

p-DNB, DNT, m-DNB, m-NP and DNP) and PhOH were added to TTTPT and TTDAT dispersions, respectively. The fluorescence of TTTPT and TTDAT was strongly quenched by TNP. In contrast, fluorescence intensities of TTTPT and TTDAT were not obvious changes after other NACs and PhOH were added. The results indicated that TTTPT and TTDAT are well selective for detecting TNP [1,33–35].

In order to check the selectivity of TTTPT and TTDAT for the actual detection of TNP, the competitive experiments were actualized in the presence of the various competitive NACs and PhOH with a concentration of 5.0×10^{-4} and 2.5×10^{-5} mol l^{-1} for the dispersions of TTTPT and TTDAT, respectively. The changes of fluorescence intensities of TTTPT and TTDAT were monitored upon addition of TNP in the presence of other NACs and PhOH. As is seen from figure 4 (green bar), neither of the other NACs nor PhOH have interferences with TTTPT detecting TNP except to DNP. Similarly, the anti-interference of TTDAT towards TNP was further validated. The results further showed that TTTPT and TTDAT are well selective for detecting TNP, indicating that the fluorescence intensities of TTTPT or TTDAT were slightly affected by the addition of other NACs and PhOH, and TTTPT and TTDAT dispersions have the excellent anti-interference ability [1,6].

2.4 *Fluorescence sensing mechanisms*

The S–V plots are non-linear with increasing concentrations of TNP and DNP (figure 3c), indicating that the static quenching processes coexists synchronously with the dynamical quenching processes during the detecting processes [6,9,36].

In order to comprehend the cause of the TTTPT or TTDAT selectivity to TNP, we measured the UV–Vis spectra of NACs and PhOH and compared them with the fluorescence spectra of the two CMPs, and employed the resonance energy transfer mechanisms, absorption competition quenching mechanism and photoinduced electron transfer mechanisms to explain the sensing mechanisms [6,33]. Except for DNP, the UV–Vis spectra of NACs and PhOH hardly overlap the fluorescence emission spectrum of TTTPT, implying that there is no resonance energy transfer process happening in the sensing process (figure 5a). The second mechanism for the quenching may be absorption competition quenching mechanism, which arises from the absorption of the excitation and emission lights of the fluorescent matter or both simultaneously by other absorbents in the detection system [7,37]. According to the UV–vis absorption spectra of phenolic NACs such as TNP, DNP, o-NP, p-NP, and m-NP, the absorption peaks of the phenolic NACs have obvious overlapping with the excitation spectrum of TTTPT (the excitation wavelength 460 nm is included). Hence, the absorption of the phenolic NACs may permeate the light adsorbed by TTTPT, resulting in fluorescence quenching [7]. As shown in figure 5b, there are overlaps among the UV–vis absorption spectra of TNP, DNP, DNT, m-NP, p-NP and o-NP with the fluorescence emission spectrum of TTDAT, which showed that there are energy transfer among TTDAT with TNP, DNP, DNT, m-NP, p-NP and o-NP [33]. The fluorescence excitation spectrum of TTDAT has overlaid evidently with the UV–vis absorption spectra of all the NACs and PhOH, which implies that there are absorption competition quenching mechanisms among TTDAT and all NACs as well as PhOH [7].

If the lowest unoccupied molecular orbital (LUMO) energy levels of the CMPs are higher than that of the analytes, the exciting electrons will transfer from CMPs to the analytes, and then perform fluorescence quenching, which is the photoinduced electron transfer quenching pathway [33].

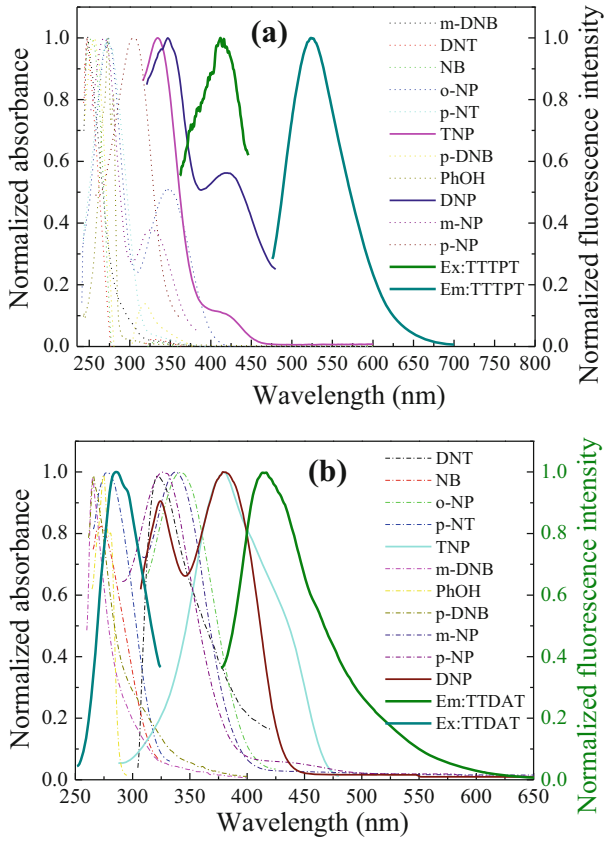

Figure 5. The absorption spectra of DNT, NB, NT, TNP, o-NP, PhOH, m-DNB, p-DNB, DNP, m-NP, p-NP as well as the emission spectra of (**a**) TTTPT (λ_{ex} = 460 nm, in DOX) and (**b**) TTDAT (λ_{ex} = 350 nm, in DMF).

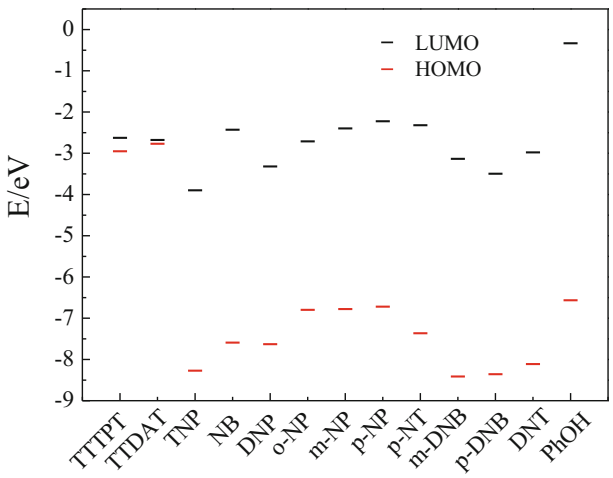

Figure 6. HOMO and LUMO calculations for CMPs, the NACs and PhOH. All the molecular orbital calculations were performed with the Gaussian 09 program at the B3LYP/6-31G* level.

Therefore, the HOMO and LUMO energy levels of TTTPT, TTDAT, the NACs and PhOH had been calculated (figure 6). The LUMO energy levels of TTTPT or TTDAT are lower than these of NB, p-NT and PhOH, which would hinder the radiative transition from TTTPT or TTDAT to NB, p-NT and PhOH, thus, there is no effective fluorescence quenching [8,21,33]. The LUMO energy levels of the TTTPT or TTDAT are higher than those of some NACs (such as TNP, p-DNB, DNP, m-DNB, o-NP and DNT), which promotes the electrons transferring from TTTPT or TTDAT to the electron-deficient NACs, and causes the fluorescence quenching phenomenon (figure 6) [9,18,33,35,38]. Because the LUMO energy level of TNP is very lower than those of the other NACs and PhOH, TNP can quench more efficiently the fluorescence of TTTPT or TTDAT than other NACs and PhOH [35].

3. Conclusions

The fluorescent tetraphenylethylene-based conjugated microporous polymers containing triphenylamine and s-triazine units (TTTPT and TTDAT) were successfully used for fluorescence sensing TNP and dinitrophenol. Both TTTPT and TTDAT have the high sensitivity for TNP with quenching constants (K_{SV}) of 1.66×10^4 and 1.31×10^5 l mol^{-1}. TTTPT can also sense dinitrophenol with the K_{SV} of 2.70×10^4 l mol^{-1}. The fluorescent quenching mechanisms of TTTPT and TTDAT for selective detecting TNP were also studied by experiments and theoretical calculations, which could attribute to the conventional photoinduced electron-transfer mechanism, absorption competition quenching mechanism and/or the resonant energy transfer mechanism.

Acknowledgements

This work was supported by the Natural Science Foundation of Anhui Education Department (under Grant No. KJ2020A0887 and KJ2018A0319), Youth Talent Fund Key Projects of Anhui Education Department (under Grant No. gxyqZD2019114), and the Open Fund of AnHui Province Key Laboratory of Optoelectronic and Magnetism Functional Materials supported (under Grant No. ZD2021001).

References

[1] Li W T, Hu Z J, Meng J, Zhang X, Gao W, Chen M L *et al* 2021 *J. Hazard. Mater.* **411** 125021
[2] Wang M, Zhang H T, Guo L and Cao D P 2018 *Sens. Actuators B-Chem.* **274** 102
[3] Wang K, Wang W J, Pan S H, Fu Y M, Dong B and Wang H 2020 *Appl. Mater. Today* **19** 100550
[4] Wang M, Gao M J, Deng L L, Kang X, Zhang K L, Fu Q F *et al* 2020 *Microchem. J.* **154** 104590
[5] Kaleeswara D and Murugavel R 2018 *J. Chem. Sci.* **130** 1

[6] Jiang N, Li G F, Che W L, Zhu D X, Su Z M and Bryce M R 2018 *J. Mater. Chem. C* **41** 11162
[7] Sun R X, Huo X J, Lu H, Feng S Y, Wang D X and Liu H Z 2018 *Sens. Actuators B-Chem.* **265** 476
[8] Dong W Y, Ma Z H, Duan Q and Fei T 2018 *Dyes Pigm.* **159** 128
[9] Saumya K and Veettil S C 2019 *J. Photochem. Photobiol. A* **371** 414
[10] Wang S, Liu Y H, Yu Y, Du J F, Cui Y Z, Song X W *et al* 2018 *New J. Chem.* **42** 9482
[11] Mothika V S, Räupke A, Brinkmann K O, Riedl T, Brunklaus G and Scherf U 2018 *ACS Appl. Nano Mater.* **11** 6483
[12] Yang X L, Hu D Y, Chen Q, Li L, Li P X, Ren S B *et al* 2019 *Inorg. Chem. Commun.* **107** 107453
[13] Geng T M, Zhang C, Chen G F, Ma L Z, Zhang W Y and Xia H Y 2019 *Micropor. Mesopor. Mat.* **284** 468
[14] Guo L, Cao D P, Yun J M and Zeng X F 2017 *Sens. Actuators B-Chem.* **243** 753
[15] Geng T M, Zhu Z M, Wang X, Xia H Y, Wang Y and Li D K 2017 *Sens. Actuators B-Chem.* **244** 334
[16] Zhang P, Guo J and Wang C C 2012 *J. Mater. Chem.* **22** 21426
[17] Liu X M, Xu Y H and Jiang D L 2012 *J. Am. Chem. Soc.* **134** 8738
[18] Li Y K, Bi S M, Liu F, Wu S Y, Hu J, Wang L M *et al* 2015 *J. Mater. Chem. C* **3** 6876
[19] Lin G Q, Ding H M, Yuan D Q, Wang B S and Wang C 2016 *J. Am. Chem. Soc.* **138** 3302
[20] Gomes R and Bhaumik A 2016 *RSC Adv.* **6** 28047
[21] Geng T M, Liu M, Zhang C, Hu C and Xia H Y 2020 *Polym. Adv. Technol.* **6** 1388
[22] Geng T M, Ye S N, Wang Y, Zhu H, Wang X and Liu X 2017 *Talanta* **165** 282
[23] Geng T M, Zhu Z M, Zhang W Y and Wang Y 2017 *J. Mater. Chem. A* **5** 7612
[24] Geng T M, Zhu H, Song W, Zhu F and Wang Y 2016 *J. Mater. Sci.* **51** 4104
[25] Geng T M, Li D K, Zhu Z M, Guan Y B and Wang Y 2016 *Micropor. Mesopor. Mater.* **231** 92
[26] Sang N N, Zhan C X and Cao D P 2015 *J. Mater. Chem. A* **3** 92
[27] Gu C, Huang N, Wu Y, Xu H and Jiang D L 2015 *Angew. Chem. Int. Ed.* **54** 11540
[28] Guo L and Cao D P 2015 *J. Mater. Chem. C* **3** 8490
[29] Bandyopadhyay S, Pallavi P, Anil A G and Patra A 2015 *Polym. Chem.* **6** 3775
[30] Xiang Z H and Cao D P 2012 *Macromol. Rapid Commun.* **33** 1184
[31] Geng T M, Liu M, Hu C and Zhu H 2021 *New J. Chem.* **45** 3007
[32] Das G, Biswal B P, Kandambeth S, Venkatesh V, Kaur G, Addicoat M *et al* 2015 *Chem. Sci.* **6** 3931
[33] Wei F, Cai X Y, Nie J Q, Wang F Y, Lu C F, Yang G C *et al* 2018 *Polym. Chem.* **27** 3832
[34] Liu H Q, Wang Y, Mo W Q, Tang H L, Cheng Z Y, Chen Y *et al* 2020 *Adv. Funct. Mater.* **13** 1910275
[35] Geng T M, Zhang C, Liu M, Hu C and Chen G F 2020 *J. Mater. Chem. A* **8** 2820
[36] Deshmukh A, Bandyopadhyay S, James A and Patra A 2016 *J. Mater. Chem. C* **4** 4427
[37] Pramanik S, Zheng C, Zhang X, Emge T J and Li J 2011 *J. Am. Chem. Soc.* **133** 4153
[38] Chen Z, Chen M, Yu Y L and Wu L M 2017 *Chem. Commun.* **53** 1989